HYDROLOGICAL PROCESSES
Hydrol. Process. **25**, 3061–3075 (2011)
Published online 12 May 2011 in Wiley Online Library
(wileyonlinelibrary.com) DOI: 10.1002/hyp.8123

Connectivity and runoff dynamics in heterogeneous basins

R. W. Phillips,[1] C. Spence[2]* and J. W. Pomeroy[1]

[1] *Centre for Hydrology, University of Saskatchewan, 117 Science Place, Saskatoon, SK, CANADA, S7N 5C8*
[2] *Environment Canada, 11 Innovation Boulevard, Saskatoon, SK, CANADA S7N 3H5*

Abstract:

A drainage basin's runoff response can be determined by the connectivity of generated runoff to the stream network and the connectivity of the downstream drainage network. The connectivity of a drainage basin modulates its ability to produce streamflow and respond to precipitation events and is a function of the complex and variable storage capacities throughout the drainage basin and along the drainage network. An improved means to measure and account for the dynamics of stream network connectivity at the catchment scale is needed to predict basin scale streamflow. At a 150 km^2 subarctic Precambrian Shield catchment where the poorly drained heterogeneous mosaic of lakes, exposed bedrock, and soil filled areas creates variable contributing areas, hydrological connectivity was measured in 11 sub-basins with a particular focus on three representative sub-basins. The three sub-basins, although of similar relative size, vary considerably in the dominant typology and topology of their constituent elements. At a 10-m spatial resolution, saturated areas were mapped using both multispectral satellite imagery and onsite measurements of storage according to land cover. To measure basin-scale hydrological connectivity, the drainage network was represented using graph theory where stream reaches are 'edges' connecting sub-basin 'nodes'. The overall hydrological connectivity of the stream network was described as the ratio of actively flowing relative to potentially flowing stream reaches. The hydrological connectivity of the stream network to the outlet was described as the ratio of actively flowing stream reaches that were connected to the outlet to the potentially flowing stream reaches. Hydrological connectivity was then related to daily average streamflow and basin runoff ratio. Improved understanding of causal factors for the variable streamflow response to runoff generation in this environment will serve as a first step towards improved streamflow prediction in formerly glaciated landscapes, especially in small ungauged basins. Copyright © 2011 John Wiley & Sons, Ltd.

KEY WORDS hydrological connectivity; heterogeneity; runoff; lakes; drainage network; variable contributing area; Canadian Shield

Received 3 September 2010; Accepted 21 March 2011

INTRODUCTION

Throughout nature, responses from heterogeneous systems are typically characterized by one or more critical internal thresholds that govern the behaviour of the whole (Sahimi, 1994; Stauffer and Ahorony, 1994; Urban and Keitt, 2001). The presence of these thresholds creates nonlinear and hysteretic connectivity among the heterogeneous components. Connectivity is a mature analytical concept in some fields, notably landscape ecology (Goodwin, 2003; Kindlmann and Burel, 2008). In hydrology, however, the definition and practical application of the term 'hydrological connectivity' has been ambiguous and varied. In a review of 'hydrological connectivity', Ali and Roy (2009) found that it has been used to define: (1) Attributes of the water cycle and its components, (2) Geomorphological or landscape features, (3) Hydrological properties, or (4) Flow processes. Hydrologists should be interested in connectivity in its functional sense so that connectivity should be considered as a measure of whether or not constituent parts of the catchment can transfer water through the available drainage network. Bracken and Croke (2007) aptly defined hydrological connectivity as the ability to transfer water from one part of a landscape to another. The hydrological connectivity of a drainage network can be conceptualized as a dependent state variable controlled by several factors that are both static and dynamic. The static factors influencing connectivity are implicitly linked to the overall catchment pattern which is governed by its composition of structural elements and the manner in which they are configured (Schröder, 2006). Therefore, the primary static controls are those Buttle (2006) proposed as the primary controls on streamflow generation. The typology of hydrological elements influences the relative predominance of hydrological processes (Allan and Roulet, 1994; Buttle, 2006; McGuire and McDonnell, 2010), threshold storage capacities and residence times. The topology of elements influences the probability of connection and relative role in runoff response (Woo and Mielko, 2007; Spence, 2007; Lane *et al*., 2009). The topography dictates the gradients and path of the network of potential hydrological connections. The key dynamic factors influencing connectivity are the relative rates of hydrological processes (Spence, 2006; Woo and Mielko, 2007; Jencso *et al*., 2010) and variation in the energy required to drive these processes (Pomeroy *et al*., 2003; Quinton and Carey, 2008).

* Correspondence to: C. Spence, Environment Canada, 11 Innovation Boulevard, Saskatoon, SK, CANADA S7N 3H5.
E-mail: chris.spence@ec.gc.ca

In hydrology, storage thresholds at multiple spatial scales have been repeatedly identified as an important factor in determining the nature of hydrological connectivity (reviewed in Spence, 2010). Hydrological connectivity has been shown to be important to nonlinear runoff response at the hillslope scale in a wide variety of landscapes including the boreal plains (Quinton *et al*., 2003), Precambrian Shield (Spence and Woo, 2002; Buttle *et al*., 2004; Mielko and Woo, 2006; James and Roulet, 2007), prairie and rangelands (Western *et al*., 2001; Fang *et al*., 2010) and temperate forests (Tromp van Meerveld and McDonnell, 2006; Lehmann *et al*., 2007). Some aspects of the concept of hydrological connectivity have been incorporated into models (Reaney *et al*., 2006; Pomeroy *et al*., 2007; Fang *et al*., 2010). However, hydrological connectivity has not been explicitly measured and accounted for at the basin scale. An improved means to measure and account for the dynamics of stream network connectivity is necessary to improve understanding of nonlinear runoff response and further advance model structure and improve streamflow prediction to better support water management decisions.

Hydrological connectivity is crucial for understanding runoff response at the larger basin scale because: (1) The topographic bounds of a basin constitute the gross drainage area but not necessarily the contributing area, and (2) The stream network that actually conveys water is rarely synonymous with the drainage network which is made up of all potential streams. As a result, active areas which are saturated and can generate runoff, are not necessarily contributing areas which are active and hydrologically connected to the outlet (Ambroise, 2004). All points within the gross drainage area could contribute runoff to the outlet of the catchment if they were saturated and connected to the outlet by other saturated areas or flow pathways. Non-contributing active areas generate runoff which is transferred downstream but does not reach the outlet. In its fully connected state, the stream network is synonymous with the drainage network, has one component and runoff from all areas may be transmitted through the drainage network to the basin outlet. When storage deficits occur within the catchment and along the drainage network, the stream network is segmented into one component connected to the outlet and one or more internally drained components not connected to the outlet.

Understanding basin-scale connectivity and its role in streamflow generation requires a quantitative analysis of the spatial and temporal patterns of stream networks, active and contributing areas. A measurement of basin scale connectivity could provide a quantitative expression of the ability of the drainage network to transfer water from one point in the catchment to another. Recent studies of hydrological connectivity have often been conducted at a small scale and have focused on the spatial connectivity of hydrological properties (Western *et al*., 2001; James and Roulet, 2007; Lehman *et al*., 2007 Detty and McGuire, 2010). Research at the basin scale has begun quantifying connectivity according to the magnitude and duration of which upstream areas are connected the stream (Jensco *et al*., 2009). In this paper, a measure of basin-scale connectivity is introduced that uses aspects of graph theory (Chartrand, 1977; Gross and Yellen, 2006) to describe the potential drainage network and active stream network from which connectivity is measured while accommodating the heterogeneity of the landscape. Using these measures of connectivity, the objectives of this paper are to investigate: (1) The dynamics of connectivity throughout a summer season, (2) The influence of connectivity on streamflow, and (3) The influence of connectivity on the streamflow response to rainfall events.

STUDY SITE

The three distinctive sub-catchments within the Baker Creek Research Basin (centre at 62° 35′N, 114° 26′W) used as the site for this study are presented in Figure 1 and Table I. Eagle Pass Creek (not its official name), Trail Creek (not its official name), and Baker Creek below Duckfish Lake, each drain 21, 8, and 25 km^2, respectively. These catchments are located in the Great Slave Upland High Boreal Ecoregion (Ecosystem Classification Group, 2008) and the Slave structural province of the Precambrian Shield (Kerr and Wilson, 2003). Total relief in each watershed is low and varies from 16 to 35 m (Table I). The terrestrial landscape can be divided into five common land covers: coniferous forest, deciduous forest, open peatlands, wetlands, and exposed bedrock (Figure 1). The fraction of each land cover differs for each basin (Table I). Forest soil profiles are typically a thin organic layer overlying mineral soil (Ecosystem Classification Group, 2008). Open peatlands situated in depressions in the rolling bedrock consist of a layer of peat approximately 1·2 m deep overlying bedrock. Wetlands have an organic layer (Ecosystem Classification Group, 2008) averaging 0·4 m in depth over glaciolacustrine deposits. The bedrock surface is moderately to highly fractured with silty sandy soils from the weathering and erosion of bedrock filling some cracks. Permafrost is discontinuous and absent from exposed bedrock, well drained areas, and areas adjacent to water courses (Wolfe, 1998). There are on average, 30 lakes in each watershed that cover approximately 6, 16, and 23% of the Trail, Eagle Pass, and Baker Creek below Duckfish basins, respectively (Table I). The Trail Creek drainage network contains the smallest lakes, on average, in the three basins. The drainage network of Baker Creek below Duckfish Lake is dominated by the 6 km^2 Duckfish Lake immediately upstream of the gauging site. Eagle Pass Creek is a chain of lakes connected by short channels.

The climate is considered semi-arid and subarctic characterized by long cold winters and short cool summers.

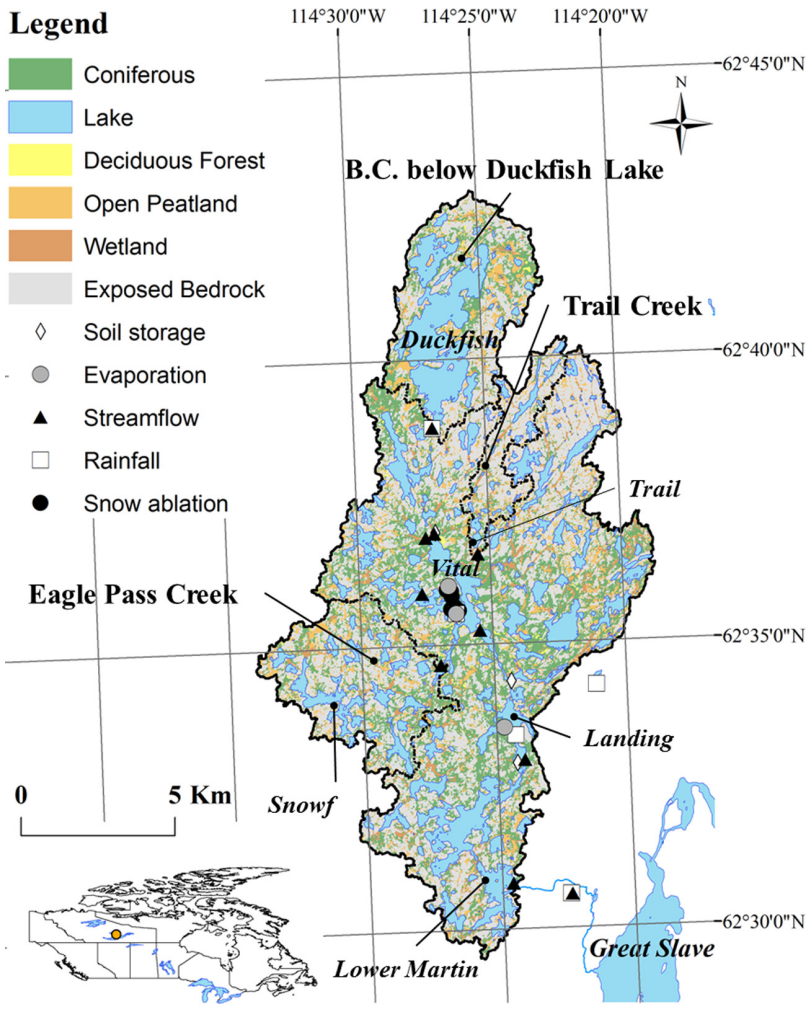

Figure 1. Baker Creek Research Basin land cover (SPOT MS satellite imagery 24 May 2008 and 20 June 2009 composite) and instrument locations

Table I. Physical characteristics of study basins. For reference, values are included for Baker Creek as a whole

	Area (km^2)	Relief (m)	Coniferous forest (%)	Lake (%)	Deciduous forest (%)	Open peatland (%)	Wetland (%)	Exposed bedrock (%)	Number of lakes	Mean lake area (m^2)
Trail Creek	8	46	4	6	0	6	3	82	27	39,786
Eagle Pass Creek	21	28	25	16	1	11	5	43	31	120,577
B.C. below Duckfish Lake	25	35	14	23	0	9	2	52	31	279,306
B.C. below Lower Martin Lake	153	65	21	23	1	10	6	40	349	88,800

The mean January temperature is −26·8 °C and the mean July temperature is 16·8 °C. Mean annual precipitation at the Yellowknife Airport (5 km south) is 281 mm of which 165 mm falls as rain and 152 mm falls as snow.

METHODS

Gross drainage area and drainage network

The gross drainage area, five hectare sub-catchments and drainage network were derived from a 1-m LiDAR digital elevation model (DEM) re-sampled to a 10-m spatial resolution for computational efficiency. A graph network, a description of a system as nodes and edges, was built from the land cover and drainage network (Gross and Yellen, 2006). In a graph network, nodes represent a system's parts, and edges represent some relationship between the parts. The nodes were defined as five-hectare headwater terrestrial sub-catchments, five-hectare receiving terrestrial sub-catchments, and lakes. At the study site, five hectares is the minimum area required to support sustained surface flows. The edges were defined as the streams connecting the nodes. Land cover was mapped using a maximum likelihood supervised classification of a composite image that combined two SPOT5 MS satellite images collected on 24 May 2008 prior to the emergence of leaves, and on 20 June 2009 following leaf out. The four multispectral bands

and the normalized difference vegetation index, NDVI (McFeeters, 1996), of both images were used as input information. Following classification, a mode-based filter with a 3 cell × 3 cell mask was passed over the image to filter out errors commonly experienced at edges due to mixed pixel signatures. The accuracy of the land cover classification was evaluated using a random sample of 314 points recorded during field surveys and marked with a handheld global positioning system (GPS) accurate to within ±8 m. The overall accuracy of the land cover map was 86% and the kappa coefficient (Congalton, 1991) was 0·82.

Active and contributing area

Mapping the active area, A_a (m^2), contributing area, A_c (m^2), and stream network required the mapping of storage states within the sub-catchments. Wells installed to the 2007 maximum depth of thaw at six representative sites (two each in open peatlands, wetlands and forests) were equipped with Solinst submersible pressure transducers to measure water table depth, z_w (mm), half hourly for the period April to September 2009. Water table depth was measured manually at least every two weeks at each of the sites to validate temperature-compensated pressure transducer readings. When pressure transducers were frozen beneath ice, manual measurements were taken every two days. Adjacent to each well, volumetric soil moisture content, θ ($m^3 \cdot m^{-3}$), was measured half hourly with a string of two site-specific calibrated Decagon Devices ECH_2O TE probes installed horizontally at the soil surface and at a depth of 250 mm below the ground surface. A soil-filled land cover type was considered active when the water table was equal to or greater than the elevation of the ground surface or the soil was saturated and the storage capacity, S_c, was equal to 0.

The water budget of exposed bedrock ($mm \cdot d^{-1}$) was calculated as

$$\Delta S_b = P + M_b - ET_b - I_b - Q_b \quad (1)$$

Rainfall, P, was measured with a continuously recording Texas Electronics TR-525M tipping bucket rain gauge and accumulations confirmed with a Meteorological Service of Canada Type B storage rain gauge. Snowmelt, M_b, was measured at a bedrock outcrop close to Vital Lake daily using an ablation line and snow survey methods similar to Heron and Woo (1978). Evapotranspiration over bedrock, ET_b, was measured directly with an eddy covariance system consisting of a three-dimensional sonic anemometer and an open-path gas analyser. Measurements of wind speed and water vapour content were taken at 10 Hz and fluxes calculated over a half hour period. Corrections to the eddy covariance measurements included coordinate rotation (Kaimal and Finnigan, 1994), the WPL adjustment (Webb *et al.*, 1980), and those for sonic path length, high-frequency attenuation, sensor separation (Horst, 1997; Massman, 2000) and oxygen extinction. Infiltration to bedrock, I_b, was estimated to be 1·07 $mm \cdot d^{-1}$, calculated using a parallel plate model as in Domenico and Schwartz (1998) for eight 3 m × 3 m plots of exposed bedrock. The model assumed that P and M_b inputs would first infiltrate, with any excess water evaporating at the rate defined by ET_b. Remaining water was stored until depression storage was filled and storage capacity was 0. The remainder would run off, Q_b. On a bedrock slope adjacent to Vital Lake, three weirs with contributing areas of 64, 38, and 11 m^2 were installed to observe bedrock runoff and validate the water budget model. When initially at storage capacity, the contributing area of the weirs required an application of 7·8 mm precipitation to fill depression storage and generate runoff. Accordingly, the storage capacity for bedrock was taken to be 7·8 mm, and once dry the bedrock returned to its absolute storage capacity. The daily storage capacity for a unit area of exposed bedrock, $S_{c,b}$ (mm), was calculated as the change in storage capacity from the previous day.

$$S_{c,b(t)} = S_{c,b(t-1)} + \Delta S_{b(t)} \quad (2)$$

When $S_{c,b}$ was 0, the bedrock was considered active. The bedrock model always accurately simulated days when each plot became saturated and produced runoff. These field observations were extrapolated over space using the distribution of bedrock in the SPOT land cover map.

To supplement the field observations of terrestrial storage, surface ponding was mapped on 17 May, 20 June, and 27 August 2009 using SPOT5 MS satellite imagery. All images were atmospherically corrected and prior to processing, each image was orthorectified with at least 15 ground control points producing a root mean square error of less than ±0·2 pixels. A supervised maximum likelihood classifier was used to classify saturated terrestrial, unsaturated terrestrial, snow/ice and open water areas in the base image collected on 17 May 2009. The four multispectral bands and the modified normalized difference water index, MNDWI (Xu, 2006), were used as input information. Training areas were selected based on notes and photographs taken during field work around the acquisition date. Two hundred and fourteen ground control points around Vital Lake were visited on 23–25 May 2009 for ground truthing and accuracy assessment. The accuracy assessment yielded an overall accuracy of 85% and a kappa coefficient (Congalton, 1991) of 0·75. Surface ponding was mapped for 20 June 2009 and 27 August 2009 based on change relative to the initial ponding classification. A simple differencing approach based on change in scaled NIR reflectance was used to create a binary change mask. This was used to distinguish amongst ice, water, and non-water-covered surfaces.

Lake level, $z_{w,s}$ expressed in units of metres above an arbitrary local datum (m.a.l.d.) was measured half hourly at five lakes of different sizes using submersible Solinst Levelogger Gold Model 3001 pressure transducers referenced to a Solinst Barologger (Figure 1). Lake level was manually tied to local bench marks at least once

every two weeks and more often during the spring freshet period. The threshold outlet elevation, z_T (m.a.l.d.), was also defined with manual surveys at each monitored lake. Lakes become active when z_T is exceeded and outflow is generated from detention storage, $S_{det,l}$ (mm). $S_{det,l}$ is the height of $z_{w.s}$ above z_T and lakes with $S_{det,l}$ values greater than or equal to zero were considered to be active. Daily relationships between $S_{det,l}$ and lake area, A_l, were defined and used to estimate $S_{det,l}$ in non-instrumented lakes throughout the basin. This method yields $S_{det,l}$ values within 15% of observed values at instrumented lakes.

The active and contributing stream network

Sub-catchments were considered active if runoff was generated within them. For lake sub-catchments, this was indicated by outflow. For terrestrial sub-catchments this was indicated by the presence of active areas. The active stream network was selected from the drainage network and depended on whether a node was a: (1) Headwater terrestrial sub-catchment, (2) Receiving terrestrial sub-catchment, or (3) Lake. One stream out of a terrestrial headwater sub-catchment was identified if there was a contiguous active area path downstream to the next sub-catchment or lake shoreline. Streams were identified through a receiving terrestrial sub-catchment by contiguous active area drainage paths to the next downstream sub-catchment. If a receiving sub-catchment was disconnected from upstream, its function reverted to that of a headwater sub-catchment. A simple lumped flow routing model was used to estimate where stream connections existed downstream of lakes. The emergence of a stream from a lake was identified if the transfer of $S_{det,l}$ out of the upstream lake was sufficient to overcome vertical and lateral losses while being conveyed downstream. Starting from a headwater location, the connectivity of the headwater lake to the next downstream lake was established through the routing of daily changes in lake detention storage, $\Delta S_{det,l}$ (mm).

$$\Delta S_{\mathrm{det},l_i} = S_{\mathrm{det},l_i(t)} - S_{\mathrm{det},l_i(t-1)} \tag{3}$$

$$Q_0 = \Delta S_{\mathrm{det},l_i} - \mathrm{E_{l_i}} \tag{4}$$

Lake outflow, Q_o (mm · d^{-1}), was taken to be the $\Delta S_{det,l}$ remaining after losses to lake evaporation E_l (mm·d^{-1}). The latter was estimated from daily measurements from an eddy covariance system on a rock outcrop in Landing Lake (Granger and Hedstrom, 2010).

Lateral and vertical losses during transmission through stream reaches were estimated assuming a trapezoidal channel of uniform width and depth comparable to instrumented streams in the basin (Spence *et al.*, 2010). Evapotranspiration during transmission (ET_t) was calculated using methods defined in Guan *et al.* (2010). Infiltration loss, q_L (m^3), during transmission was estimated using Darcy's law using hydraulic gradients, i (m·m^{-1}), measured near instrumented streams, hydraulic conductivities from Guan (2010).

Quantifying connectivity

The overall connectivity of the stream network is a measure in some ways analogous to antecedent moisture. The connectivity of the stream network $C_{E,N}$ was taken to be the ratio of edges in the active stream network, E_a, to the total number of edges in the drainage network E_p

$$C_{E,N} = \frac{E_a}{E_p} \tag{5}$$

The connectivity to the outlet, $C_{E,o}$, however, is a measure of the stream network's ability to transfer antecedent and event water to the outlet. The connectivity of the stream network to the outlet, $C_{E,O}$, was defined as the ratio of contributing edges, E_c, to E_p:

$$C_{E,O} = \frac{E_c}{E_p} \tag{6}$$

Streamflow and runoff response

Streamflow was observed at a total of 11 stations located at the outlets of headwater lakes, in tributaries, and in a nested fashion along Baker Creek (Figure 1). The flow at Lower Martin Lake outlet was measured at the Water Survey of Canada (WSC) hydrometric gauge 07SB013. At all other sites streamflow was measured periodically using area-velocity methods based on velocity measurements made using a SONTEK FloTracker Acoustic flow metre. Stage-discharge relationships were developed for each site from observed streamflow and corresponding manually surveyed lake levels.

To investigate the influence of connectivity on runoff response, event volume, Q_e (m^3), was estimated by separating storm flow from the hydrograph using an exponential decay function (Dingman, 1973)

$$Q_e = \int_{t_{qo}}^{t_{qe}} q - \left(q_0 \cdot e^{\left(-\frac{t}{t^*}\right)} \right) dt \tag{7}$$

where q ($m^3 \cdot s^{-1}$), is the observed daily average streamflow, q_o ($m^3 \cdot s^{-1}$) is the daily average streamflow on the day preceding rainfall, Q_e ($m^3 \cdot s^{-1}$) is the daily average streamflow on the last day of the runoff event, and t (days) is the time since the beginning of the rain event. The recession coefficient, t^*, was calculated as the reciprocal of the slope of a plot of ln(q) *versus* t for the receding limb of the hydrograph prior to interruption by the rain event (McNamara *et al.*, 1998). The runoff ratio, R_r, was calculated as

$$R_r = \frac{Q_e}{P_e + M_e} \tag{8}$$

Rainfall, P (mm), was measured with continuously recording Texas Electronics TR-525M tipping bucket rain gauges at three sites in the Baker Creek Research Basin and at two sites located just outside the basin boundary (Figure 1). Meteorological Service of Canada Type B manual rain gauges were used at four of the five sampling points to validate tipping bucket measurements. The error

observed between the cumulative precipitation measured by the tipping bucket and Type B rain gauges was −2, 5, 5 and 3%, respectively. Sub-basin rainfall was estimated using Thiessen polygons around the five precipitation measurement sites. Melt, M (mm), was measured using ablation lines and methods similar to Heron and Woo (1978) at one site for each land cover located around Vital Lake (Figure 1). Daily melt was calculated for each sub-basin as the product of the daily melt in a land cover, the observed snow covered fraction in that land cover, and the area of the land cover within the sub-basin. Sub-basin inputs for a given runoff event were taken to be sum of rainfall for the event, P_e (m^3), and snowmelt for the event, M_e (m^3).

RESULTS

Streamflow

The level of Trail Lake rose above its debris dam on 30 April and streamflow rose sharply to a peak of 0·124 $m^3 \cdot s^{-1}$ on 4 May (Figure 2). The Eagle Pass Creek sub-basin began flowing at its outlet on 4 May and peaked at 0·274 $m^3 \cdot s^1$ on 12 May (Figure 2). Duckfish Lake maintained connection throughout the winter of 2008–2009 and was flowing before the spring freshet. Duckfish Lake peaked at 0·159 $m^3 \cdot s^{-1}$ on 20 May. The recession of Trail Creek flow was abrupt and streamflow fell sharply through the spring (Figure 2). The level of Trail Lake declined to the outlet's debris dam elevation on 18 June and flow dropped to 0·021 $m^3 \cdot s^{-1}$. Following a short-term response to the 23 June and 1–3 July rainfall events, Trail Lake once again fell below its debris dam on 13 July and flow slowed to less than 0·016 $m^3 \cdot s^{-1}$ for the duration of the study period. Eagle Pass Creek's spring recession was gradual and interrupted by responses to even small rainfall events (Figures 2). The recession of flow in Baker Creek below Duckfish Lake was gradual through the spring but grew steeper as evapotranspiration and infiltration losses increased during summer (Figure 2). At the end of September, several small rainfall events occurred in close succession and caused streamflow to rise in the Duckfish Lake and Eagle Pass Creek sub-basins (Figure 2). The level of Trail Lake rose but only reached the level of its debris dam on 1 October and as a result, a rise in streamflow was not observed (Figure 2).

Dynamics of active and contributing area and the stream network

Much of the lake controlled stream network was disconnected at the beginning of the 2009 water year. The melt period began on 10 April and on 9 May all terrestrial land covers were active (Figure 3). Lake storage capacity was overcome and active and contributing areas were the same as the gross drainage area (Figures 4, 5, 6, and 7, Table II) while the stream network was synonymous with the drainage network (Figure 8). The majority of forest and exposed bedrock areas became inactive on 11 and

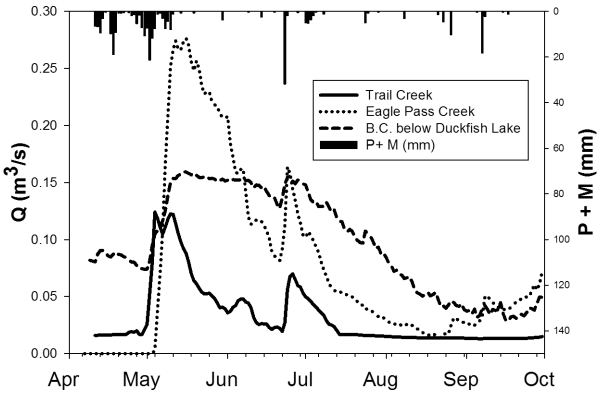

Figure 2. The 2009 streamflow hydrographs for Trail Creek, Eagle Pass Creek, and Baker Creek below Duckfish Lake sub-basins as well as rainfall (P) and snowmelt (M) inputs during 2009. P and M presented in this plot were measured near Vital Lake. Although rainfall is variable throughout the basin, the plot presented here for all of Baker Creek serves as a valid approximation of the timing and rough magnitude of rain events during 2009. Values unique to each study basin were used in analysis of runoff response

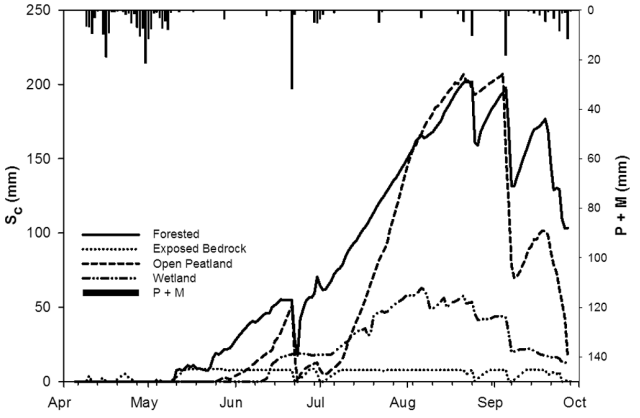

Figure 3. Storage capacity (S_c) for terrestrial land covers as well as rainfall (P) and snowmelt (M) inputs during 2009. 9 May, 17 May, 20 June, and 27 August 2009 the dates when overall stream network connectivity and connectivity to the outlet were sampled are indicated by vertical lines

12 May, respectively (Figure 3), causing a small number of headwater terrestrial sub-catchments to disconnect. By 17 May, active area and contributing area had fallen (Figure 7 and Table II) as large tracts of forest and exposed bedrock became inactive. However, storage capacity remained satisfied in peatlands (Figure 3) and headwater lakes and $C_{E,O}$ and $C_{E,N}$ remained high (Figure 8).

Rainfall during the spring was light (12 mm) and losses to evapotranspiration and runoff caused an increase in S_c for all land covers (Figure 3). Peatlands became inactive on May 27 and wetlands on June 11 (Figure 3). Open peatland and wetland land covers were not completely inundated but partial surface ponding was still regionally prolific and was captured through remote sensing (Figures 4–6). Storage capacity in key terrestrial elements such as peatlands (Figure 3) resulted in the widespread disconnection of headwater terrestrial sub-catchments from the lake controlled stream network (Figures 4–6) and inputs to headwater lakes slowed. On

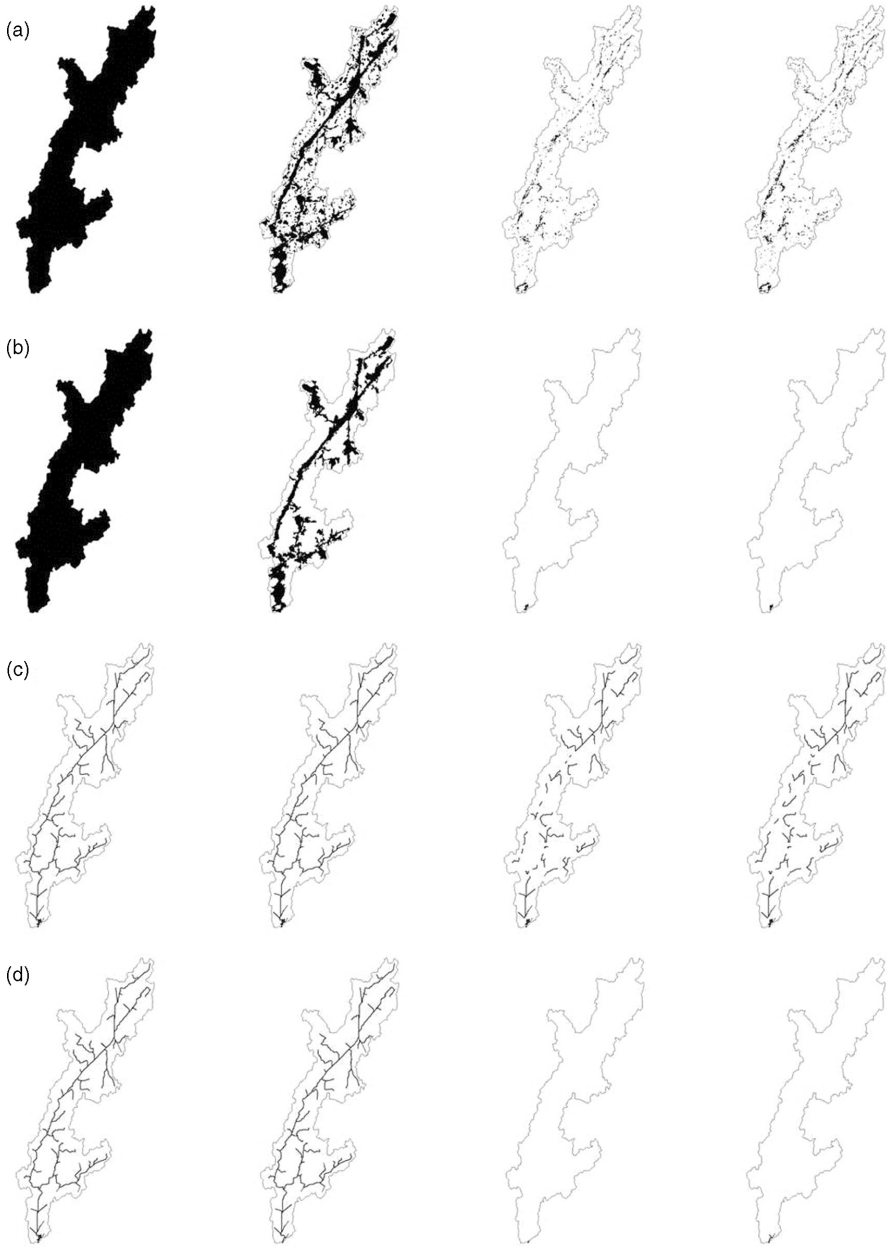

Figure 4. Trail Creek active area (a), contributing area (b), active stream network (c), and contributing stream network for (from left to right) 9 May, 17 May, 20 June, and 27 August 2009

June 14, small headwater lakes began to disconnect. The lack of inflows to receiving lakes following the disconnection of headwater lakes upstream meant that evaporation and outflow quickly reduced the remaining detention storage and the lake controlled stream network quickly disintegrated. By 20 June, $C_{E,N}$ and $C_{E,O}$ had dropped significantly (Figures 4–6 and 8). In the Trail Creek sub-basin, unlike the peatlands, the channel wetlands between receiving lakes remained inundated and active (Figure 4). However, lakes with levels below their outlet elevation caused the disintegration of the stream network (Figure 4) and A_c decreased to a minor wetland immediately upstream of the gauge site (Figures 4 and 7, Table II). Nevertheless, large headwater lakes with high volumes of detention storage and inefficient outlets were able to maintain outflow. In the central lake chain of the Eagle Pass Creek sub-basin, connectivity to the outlet was maintained throughout the summer by outflow contributed from Snowf Lake (not official name) and a large wetland complex on its northwestern shore (Figures 1 and 5). The rest of the Eagle Pass Creek sub-basin was disconnected from the outlet by headwater lakes (Figure 5). However, saturated portions of open peatlands upstream of these headwater lakes (Figure 5) kept $C_{E,N}$ higher than in the other two study basins by maintaining the connectivity of upland sub-catchments through the summer (Figure 8, Table II). In the Duckfish Lake sub-basin, the large peatland and wetland complexes in the northeast of the sub-basin (Figure 1) became inactive and disconnected outlying areas from the outlet (Figure 6). The contributing stream network was limited

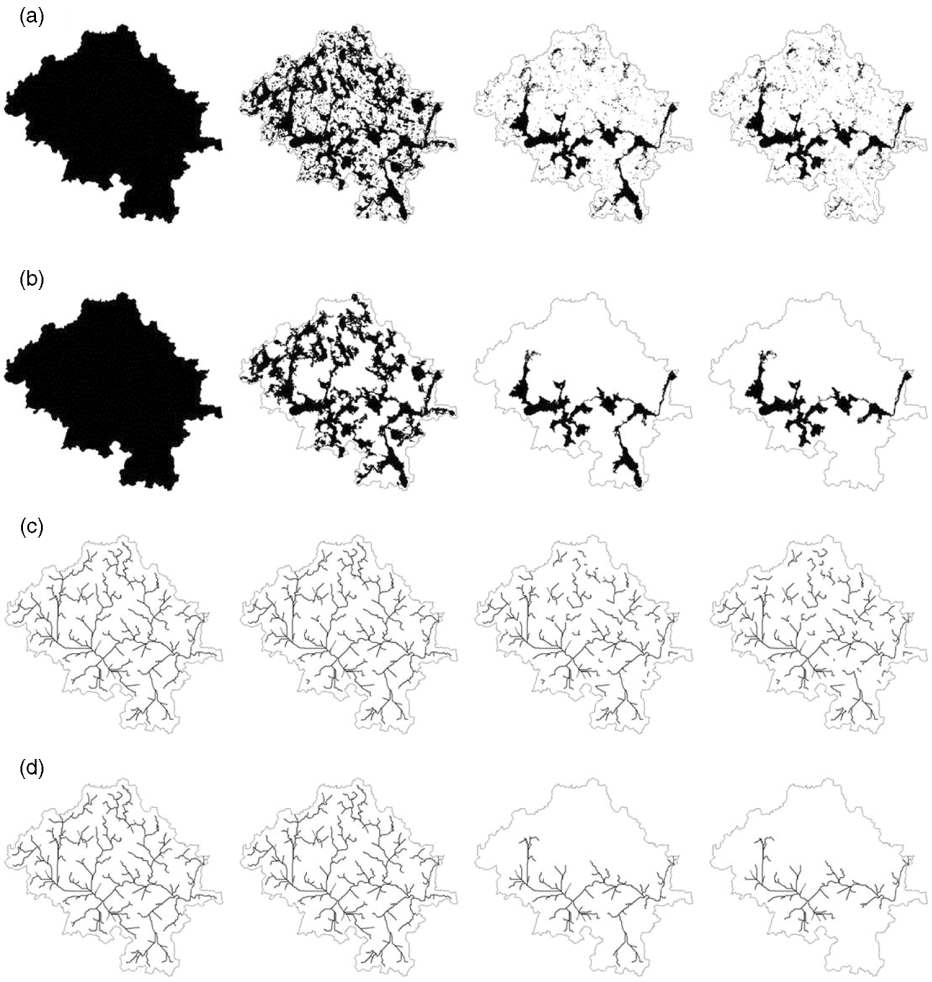

Figure 5. Eagle Pass Creek active area (a), contributing area (b), active stream network (c), and contributing stream network for (from left to right) 9 May, 17 May, 20 June, and 27 August 2009

to Duckfish Lake and its surrounding shoreline (Figure 6 and 8).

A rainfall of 34 mm fell on 23 June and was sufficient to fill the S_c of exposed bedrock, open peatlands and both headwater and receiving lakes (Figure 3). The stream network reintegrated starting with headwater terrestrial subcatchments in which bedrock was dominant and where reactivated peatlands permitted water to cascade downstream to the drainage network's core lake chains. The runoff driven flood wave reestablished the connectivity of the stream network and resulted in a streamflow response at each outlet (Figure 2). Through July and August, S_c increased in all terrestrial land covers (Figure 3) and inactive lakes due to evapotranspiration exceeding precipitation. On 27 August, the active stream network remained largely disconnected (Figures 4–6) and $C_{E,O}$ was low (Figure 8). The state of the terrestrial land covers was generally inactive and all lakes except for those downstream of Duckfish Lake and Snowf Lake were inactive (Figures 4–6). A rainfall of 21 mm on 6 September filled S_c in the exposed bedrock and reduced it in other land covers (Figure 3). The 6 September rainfall event was insufficient to reestablish the lake controlled stream network and streamflow response was minimal in all sub-basins except Eagle Pass Creek (Figure 2). As the instrumentation was removed at the end of September, a succession of smaller rain events was gradually filling S_c in all terrestrial land covers (Figure 3).

Connectivity and streamflow

Between 9 and 17 May, connectivity remained high in all three study basins. Over this period flow increased in Eagle Pass Creek and Baker Creek below Duckfish Lake while decreasing slightly in Trail Creek. Through the summer, the stream network disintegrated and $C_{E,O}$ decreased (Figures 4–6 and 8). As the contributing stream network contracted (Figures 4–6), the area able to contribute decreased and Q at the outlet fell. There was a general positive relationship between $C_{E,O}$ and Q (Figure 9). However, the nature of the relationship between $C_{E,O}$ and Q was observed to be different for each sub-basin (Figure 9). Trail Creek was observed to be either highly or poorly connected to its outlet. When $C_{E,O}$ was 1·0 on May 17, flow was 0·08 $m^3 \cdot s^{-1}$. When poorly connected, $C_{E,O}$ was less than 0·03 and Q was less than 0·015 $m^3 \cdot s^{-1}$. Streamflow at the outlet of Eagle Pass Creek was observed to decrease from the high flow in spring roughly logarithmically to decreases in $C_{E,O}$

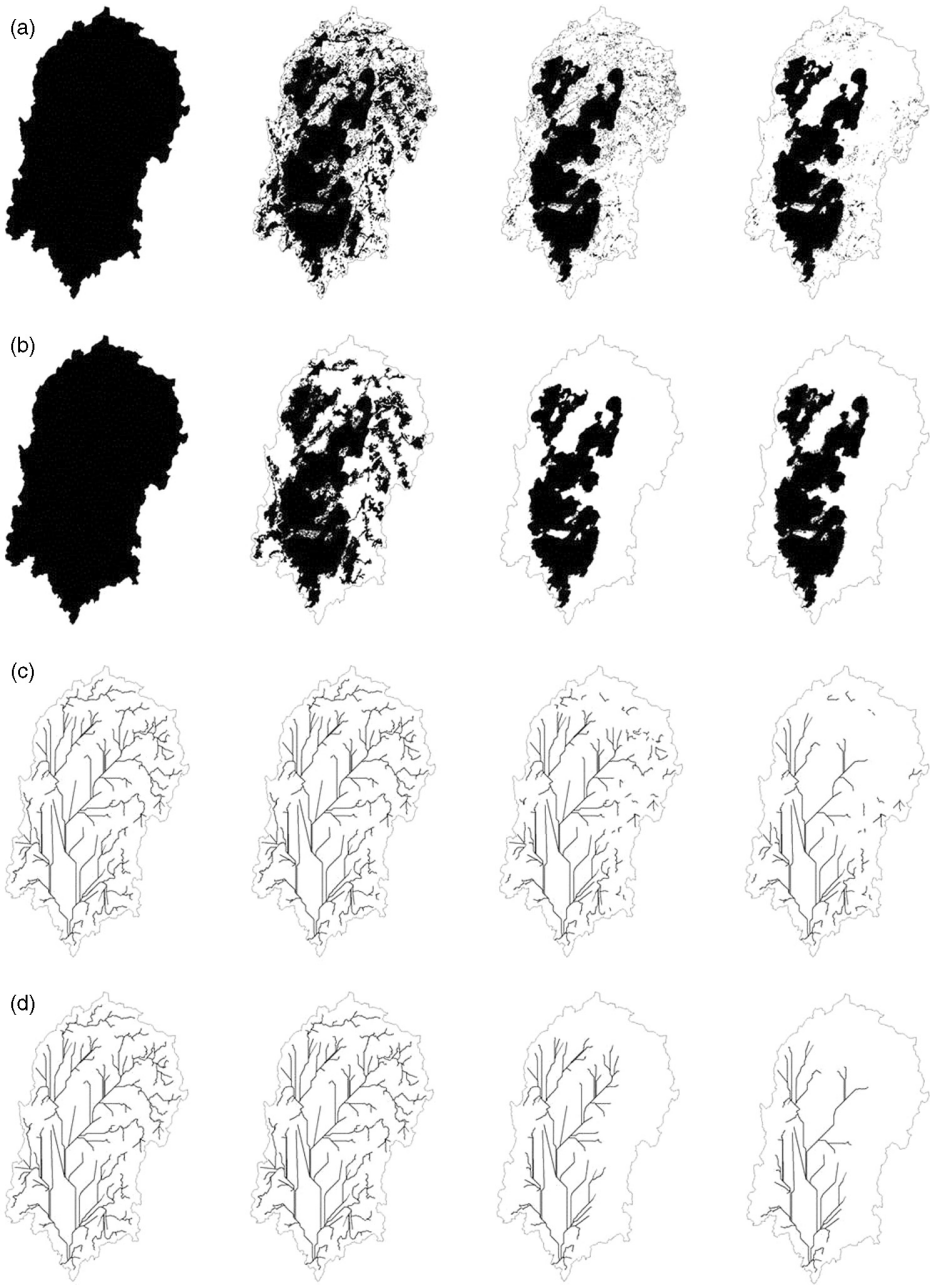

Figure 6. Baker Creek below Duckfish Lake active area (a), contributing area (b), active stream network (c), and contributing stream network for (from left to right) 9 May, 17 May, 20 June, and 27 August 2009

(Figure 9). At Duckfish Lake, $C_{E,O}$ dropped from 0·98 to 0·40 from 17 May to 20 June, but Q only decreased from 0·17 $m^3 \cdot s^{-1}$ to 0·13 $m^3 \cdot s^{-1}$. From 20 June to 27 August, $C_{E,O}$ decreased from 0·40 to 0·31, but over the same period, a decrease in Q from 0·13 $m^3 \cdot s^{-1}$ to 0·04 $m^3 \cdot s^{-1}$ was observed. As a result the relationship between $C_{E,O}$ and Q follows a logarithmic form.

Connectivity and runoff response

Responses to rainfall and melt events were examined relative to antecedent connectivity in each study basin (Figure 10, Tables II and III). On 19 May, when $C_{E,O}$ was high, a small melt event produced a response in all sub-basins that were already in recession. The slope of the recession was altered at Trail Lake yielding a Q_e of 816 m^3 with a R_r of 0·68. In the Eagle Pass sub-basin, the melt increased flow for two days yielding a Q_e of 11,840 m^3 with a R_r of 0·53. Baker Creek below Duckfish Lake responded to an input of 15 100 m^3 with a Q_e of 4730 m^3 and a R_r of 0·32. On 23 June, a rainfall of 34 mm occurred. Prior to the rain event $C_{E,O}$ was low (Figure 9), but S_c was still relatively small, especially in lakes which had recently disconnected. During the 23 June event, Trail Creek sub-basin received 243 758 m^3 and yielded 36 667 m^3 with a R_r of 0·15. Eagle Pass Creek sub-basin received 741 810 m^3 resulting in a Q_e of 70 187 m^3 with a R_r of 0·09. The Baker Creek below Duckfish Lake sub-basin received 770 037 m^3 and yielded 50 960 m^3 with a R_r of 0·07. On 6 September, a rainfall of 21 mm occurred. With the exception of

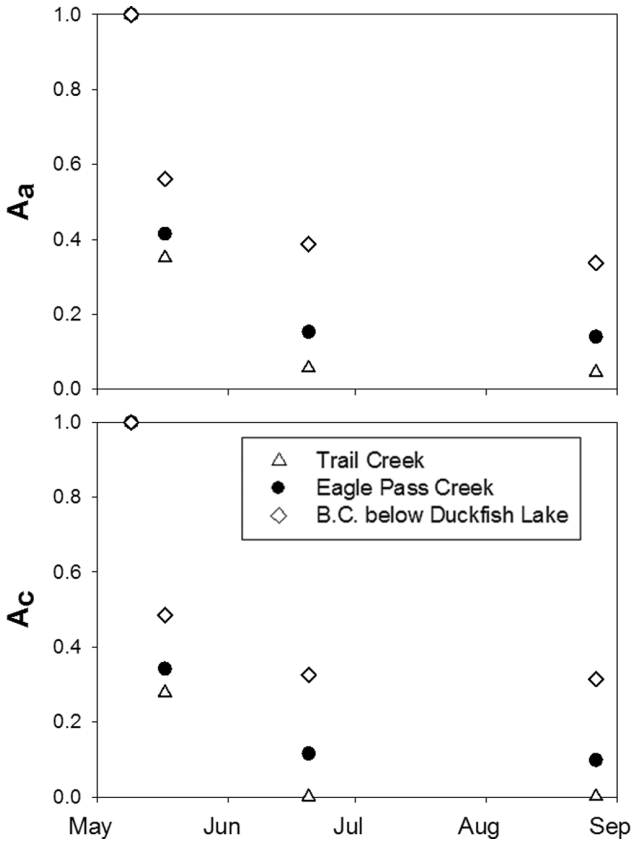

Figure 7. Active area (top) and contributing area (bottom) in the three study basins for the days listed in Table II presented as a proportion of gross drainage area

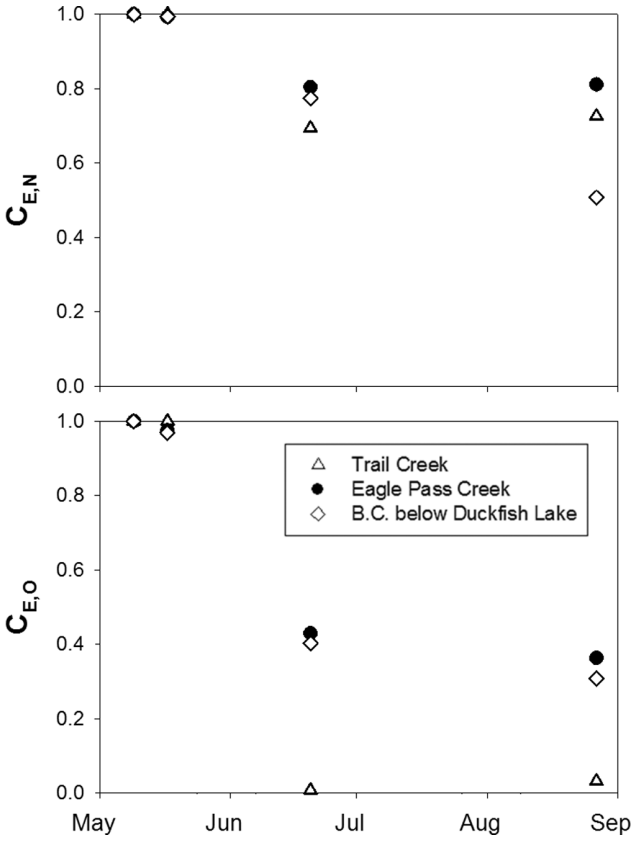

Figure 8. Overall stream network connectivity, $C_{E,N}$, (top) and connectivity to the outlet, $C_{E,O}$, (bottom) in the three study basins for the days listed in Table II. The 9 May 2009 and 17 May 2009 values were very similar for most sub-basins

the bedrock, the terrestrial land covers remained inactive during the rain event and contribution to storm flow was limited to lake chains connected to the outlet and their adjacent bedrock lake shores. The 88 568 m^3 of rainfall on the Trail Creek sub-basin produced a Q_e of only 2313 m^3 with a R_r of 0·01. On 6 September, 456 658 m^3 of rain fell on the Eagle Pass sub-basin yielding a Q_e of 26 514 m^3 with a R_r of 0·06. The Baker Creek below Duckfish Lake sub-basin received 415 216 m^3 of rain and yielded a Q_e of 4343 m^3 with a R_r of 0·01.

DISCUSSION

Connectivity dynamics

Storage states were highly dynamic and all land cover types were observed to be capable of operating as runoff sources or sinks. For a brief period during the spring, all sub-catchments were connected downstream and functioned as sources. The stream network then disintegrated as individual elements became inactive and disrupted the connectivity of the stream network. As the stream network disintegrated, it was segmented into one component connected to the outlet and one or more internally drained components that were active but not connected to the outlet. In each of the study basins this caused the divergence of A_c and A_a (Figure 7) as well as $C_{E,N}$ and $C_{E,O}$ (Figure 8) after 17 May.

Black (1997) proposed that basins could perform collecting, storing, and discharging functions. It was observed that individual elements could perform these same functions. The function of individual elements that collected and attenuated runoff was observed to drive the dynamics of basin scale connectivity. When active,

Table II. Observed active area (A_a), contributing area (A_c), connectivity to the outlet ($C_{E,O}$) and overall connectivity of the stream network ($C_{E,N}$)

Date	Trail Creek				Eagle Pass Creek				Duckfish Lake			
	09 May	17 May	20 Jun	27 Aug	09 May	17 May	20 Jun	27 Aug	09 May	17 May	20 Jun	27 Aug
Aa ($m^2 \times 10^6$)	7·84	2·75	0·44	0·36	20·66	8·58	3·17	2·90	25·16	14·13	9·74	8·49
Ac ($m^2 \times 10^6$)	7·84	2·18	0·01	0·01	20·66	7·07	2·40	2·03	25·16	12·21	8·19	7·92
$C_{E,X}$	1·00	1·00	0·69	0·73	1·00	0·99	0·80	0·81	1·00	0·99	0·77	0·51
$C_{E,O}$	1·00	1·00	0·01	0·03	1·00	0·98	0·43	0·36	1·00	0·97	0·40	0·31

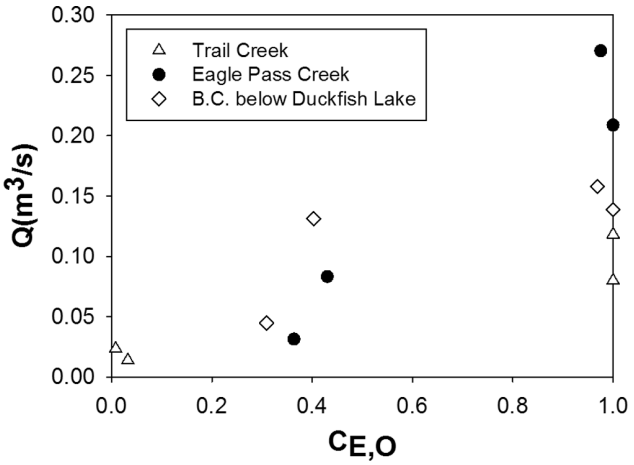

Figure 9. Daily average streamflow, Q ($m^3 \cdot s^{-1}$), on the satellite image acquisition date defined in Table II, for different states connectivity to the outlet, $C_{E,O}$, for the sub-basins of interest

they could perform all three functions, when inactive they could only collect and store. These elements controlled connectivity by acting as '*gatekeepers*' for runoff from upstream contributing areas. At Baker Creek, the open peatlands and wetlands situated in upland areas controlled the connectivity of bedrock dominated headwater catchments. Downstream lakes were gatekeepers for large tracts of headwater sub-catchments.

When active, gatekeepers facilitate the transfer of runoff contributed from headwaters both by remaining active themselves as well as maintaining the connectivity of the stream network downstream. They do so by attenuating runoff collected from upstream, storing it and slowly releasing it over time and sustaining streams downstream that would otherwise run dry. A gatekeeper's ability to remain active depends on its size and efficiency (Spence, 2007) in translating stored runoff collected from upstream to outflow as well as the intensity and duration of upstream contributions. The intensity and duration of upstream contributions to gatekeeper headwater lakes has been noted to be heavily influenced by the land cover in the areas upstream as well as the size of the lake relative to gross drainage area upstream (Mielko and Woo, 2006). Gatekeeper elements with large volumes and relatively inefficient outlets such as Duckfish Lake were able to remain active longer by attenuating large volumes of spring snowmelt. Gatekeeper elements located further downstream in the stream network were able to remain active into the summer as the duration of runoff collection from upstream was prolonged. For instance at Eagle Pass Creek, small receiving lakes located downstream Snowf Lake (Figures 1 and 5) were maintained by outflow through the summer and remained active long after headwater lakes of comparable size (Figure 5) had disconnected. The effect of a gatekeeper on $C_{E,O}$ downstream is controlled by its topology and controlled by the rate and duration of outflow. Snowf Lake, located in the headwaters of Eagle Pass Creek, maintained lake levels and connectivity downstream throughout the summer.

When inactive, gatekeeper elements disrupt connectivity and act as sinks for contributions from upstream. The area of a gatekeeper influences the amount of run-on required from upstream to become active. Storage capacity is proportional to surface area, and therefore, the larger a gatekeeper is, the greater the input volume required to reestablish connection. The topology of a gatekeeper defines the impact that its inactivity may have on $C_{E,O}$. The influence of a gatekeeper element on $C_{E,O}$ increases

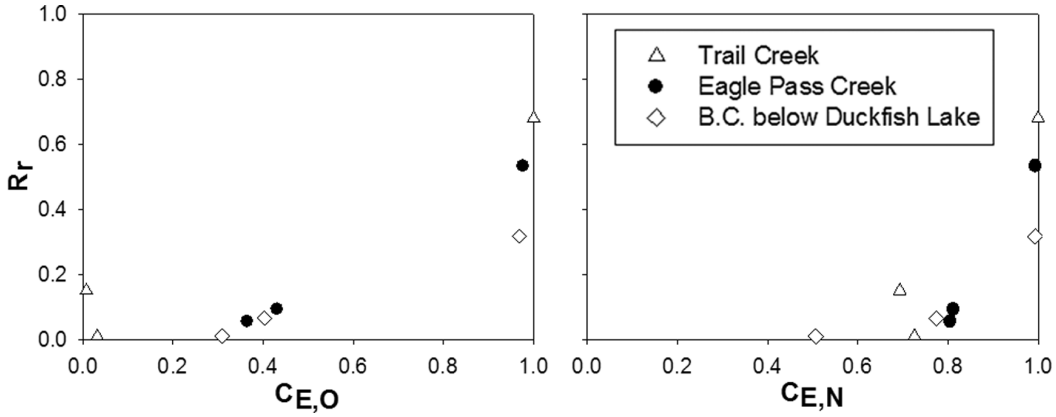

Figure 10. Runoff ratios, R_r, observed for different antecedent states of connectivity to the outlet, $C_{E,O}$, (left) and overall connectivity, $C_{E,N}$ (right)

Table III. Runoff characteristics observed for rainfall or melt events following satellite image acquisition during 2009

Date	P or M (m^3)			Q_e(m^3)			R_r		
	Trail	Eagle Pass	Duckfish	Trail	Eagle Pass	Duckfish	Trail	Eagle Pass	Duckfish
19 May 09	1,568	22,730	15,099	816	11,844	4,727	0·68	0·53	0·32
23 Jun 09	243,758	741,810	770,037	36,667	70,187	50,960	0·15	0·09	0·07
06 Sep 09	88,568	456,658	415,216	2,313	26,154	4,343	0·01	0·06	0·01

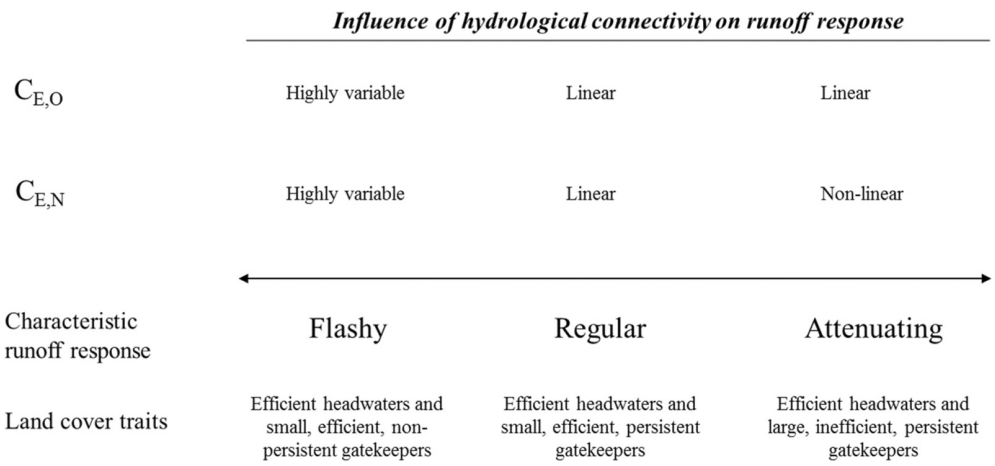

Figure 11. Basin classification according to the influence of connectivity on runoff response

the further downstream it is located. With closer proximity to the outlet, its inactivity disconnects potential contributions from an increasing number of upstream elements.

It is important to note that as upstream areas disconnect the relevant topology of downstream elements changes. As the stream network upstream became disconnected (Figures 4–6), downstream elements reverted to performing 'headwater' 'functions. This dynamic relative topology resulted in a cascading effect of disconnection; regions dominated by headwater terrestrial catchments with small efficient gatekeepers quickly disintegrated during hydrograph recession. This was particularly pronounced in the Trail Creek basin where small and efficient gatekeeper peatlands and lakes (Figure 1) caused a highly variable connectivity and highly ephemeral streamflows (Figures 2,4, and 8). This also caused the rapid disconnection of terrestrial portions outlying from the central Eagle Pass Creek lake chain (Figure 5) and Duckfish Lake (Figure 6).

Connectivity and streamflow

At high connectivity, there was a high range of streamflow values observed for each basin. At Trail Creek, $C_{E,O}$ remained at 1 while flow at its outlet receded between 9 and 17 May. Flows in both Eagle Pass Creek and Baker Creek below Duckfish Lake were still rising on 9 May and, although connectivity dropped slightly between 9 and 17 May, streamflow increased. This was the result of the simultaneous disconnection of headwater terrestrial areas and advance of the main spring freshet flood wave downstream. This showed that a highly connected stream network can support a range of flow and alludes to the potential for a possible hysteretic relationship between connectivity and streamflow. After 17 May, decreasing values of $C_{E,O}$ resulted in lower Q in the three study basins (Figure 9). However, the characteristic shape of relationships observed between Q and $C_{E,O}$ varied significantly for each sub-basin. The characteristic shape of the relationship between $C_{E,O}$ and Q was greatly influenced by the configuration and size of active areas in the stream network and relationships between storage and discharge within individual elements. At the basin scale, the active areas of particular importance to Q were lakes. In a drainage basin where the last store in the chain was small relative to upstream contributions, inflows from the contributing stream network heavily influenced lake detention storage in the outlet controlling lake and thus sub-basin outflow. For instance, Trail Lake was small relative to its upstream contributing area and did not significantly attenuate outflow. Inflows from the contributing stream network heavily influenced lake detention storage and thus sub-basin outflow. When upstream contributions were high as they were on 17 May, connectivity and flow were high. However, when connectivity was low as it typically was in summer, streamflow in the Trail Creek sub-basin was minimal (Figures 4 and 9). At Eagle Pass, lakes of similar size were distributed throughout the central lake chain and headwaters. The relationship between $C_{E,O}$ and Q at Eagle Pass was roughly logarithmic with the steepest slope of the three study basins. The headwater lakes that collect water from the hillslopes in Eagle Pass were still connected on 17 May and streamflow was high. By 20 June, many of the headwater lakes outside of the central chain had become disconnected and flow significantly decreased. Although one more lake in the south of the basin became disconnected, connectivity remained stable after 20 June and Q decreased as detention storage in the central lake chain was exhausted due to evapotranspiration and outflow. Because the lakes are all small in Eagle Pass Creek (Figure 1 and Table I), no individual lake exerted exceptional influence on the streamflow close to the outlet of the sub-basin. This was not the case for lakes that are large relative to their upstream contributions and situated close to the basin outlet. Such lakes exerted significant influence on the basin outflow and dampened any influence of upstream connectivity. This was seen at the Baker Creek below Duckfish Lake sub-basin in particular, where Duckfish Lake controlled basin outflow and caused a logarithmic relationship between Q and $C_{E,O}$. This resulted from the fact that after 20 June, the contributing portion of Baker Creek below Duckfish Lake remained stable and confined to Duckfish Lake itself and a few terrestrial sub-catchments lining

its shores (Figure 6) but the level of Duckfish Lake had dropped significantly over the same period. Because of its location and relative size, the level and stage-discharge relationship of Duckfish Lake were the primary controls on outflow from the Baker Creek below Duckfish Lake sub-basin and so, $C_{E,O}$ had little influence on Q.

Connectivity and runoff response

Generally, higher antecedent connectivity was found to result in higher R_r (Figure 10). On 19 May, antecedent connectivity was high and even small inputs were translated to streamflow at the outlet with relatively high efficiency (Figure 10 and Table II). When antecedent connectivity was low, rainfall was first directed to fill storage capacities and reestablish inactive connections before reaching the outlet. However, the relationships between runoff response and connectivity differed for each sub-basin and the emergence and magnitude of runoff response was punctuated by the importance of the magnitude of inputs relative to antecedent storage capacities in the drainage network's gatekeeper elements. Input events large enough to reestablish the connectivity of the stream network to the outlet by reactivating gatekeepers induced a streamflow response. In flashy basins (e.g. Trail Creek) ample source areas and small inactive gatekeeper elements meant that runoff response could be highly variable even when antecedent connectivity and streamflow were low. Once the bedrock areas were active, storage capacities in the relatively small gatekeeper peatlands and lakes downstream were quickly filled: the 23 June rain event was large enough to activate the bedrock and then the gatekeeper peatlands and lakes so that flow in Trail Creek rose disproportionally to the antecedent connectivity (Figure 10 and Table II). Input events that were not large enough to reestablish connectivity to the outlet did not produce a streamflow response. Smaller rain events (e.g. 6 September) only activated areas with small S_c but were not large enough to activate gatekeepers (Figure 3), so little or no response was observed at the outlet (Figures 2 and 10, Table II). The runoff response curves (Figure 10) were shaped by the relative efficiency of different portions of the drainage network in producing runoff from inputs. In Figure 10, values of $C_{E,O}$ approaching 1 are associated with connections in the headwaters of the drainage network, values closer to 0 are associated with connections in the central lake chains of the drainage network. In Eagle Pass, the relationship between R_r and $C_{E,O}$ was roughly linear and thus additional elements from the expanding contributing stream network were equally efficient at translating rainfall to runoff. This results from the distribution of small lakes of similar size throughout the drainage network that control the connectivity of the stream network. At Duckfish Lake, the relationship between $C_{E,O}$ and R_r was nearly linear but the slope of the relationship was less steep than that observed for Eagle Pass. This is likely because the influence of the headwater connections was obscured by Duckfish Lake which controlled flow out of the basin. The presence of such an element at the outlet of the basin decreases efficiency by attenuating runoff longer, prolonging the duration of the runoff event and enabling more collected runoff to be abstracted by evapotranspiration while being transmitted to the outlet.

In Figure 10, values of antecedent $C_{E,N}$ closer to 1 can be associated with connections from areas whose activity is not persistent such as headwater terrestrial subcatchments dominated by bedrock and small gatekeeper elements. Lower values of antecedent $C_{E,N}$ can be associated with elements whose inactivity is less likely. At Trail Creek, the relationship between R_r and $C_{E,N}$ shared a highly variable pattern similar to that noted between R_r and $C_{E,O}$. In distributed sub-basins where most of the inactive gatekeepers were of similar size and small like Eagle Pass, less persistent gatekeepers had a similar influence on R_r as the more persistent ones and the increase in R_r with higher $C_{E,N}$ was nearly linear (Figure 10). In the Baker Creek below Duckfish Lake sub-basin, the relationship between R_r and $C_{E,O}$ was notably nonlinear and the activity of the less persistent connections induced a greater increase in R_r than the more persistent connections. This implies that the less persistent elements in the headwaters are more efficient than Duckfish Lake at translating inputs to runoff. This relative efficiency of headwater terrestrial portions stems from the fact that the transmission of collected runoff is distributed among a large number of small gatekeepers with efficient outlets over a landscape with greater relief than further downstream. The relative inefficiency of Duckfish Lake results from the abstraction by evaporation of large volumes of collected runoff while it is stored and slowly translated to discharge through Duckfish Lake's single and relatively inefficient outlet.

Basin classification according to the influence of connectivity on runoff response

For a particular drainage basin the influence hydrological connectivity has on runoff response is controlled by five traits: (1) the efficiency of headwaters source areas, (2) the proportion of headwaters source areas, (3) the efficiency of gatekeepers, (4) the size of gatekeepers relative to upstream contributions, and (5) the ability of gatekeepers to attenuate flow. Climate would also presumably affect the influence of connectivity by dictating the magnitude, frequency, and duration of inputs to the basin. Variations in inputs could not be analysed in this study with the basins in such proximity. Figure 11 summarizes the influence that heterogeneity can have on the relationship between connectivity and runoff response. At one end of the spectrum are basins with a high proportion of efficient headwater source areas and small, efficient but non-persistent gatekeepers, which exhibit a flashy runoff response and a poor relationship between connectivity and runoff response. At the other end of the spectrum are basins with efficient headwaters and large, inefficient, persistent gatekeepers. The runoff response from such basins is attenuated and the influence of connectivity on runoff response is nonlinear. In the middle are basins with

a high proportion of efficient source areas in the headwaters, and small, efficient but persistent gatekeepers, which will have a characteristically regular runoff response and relationship between connectivity and runoff response.

CONCLUSIONS

In order to improve the understanding of connectivity dynamics in heterogeneous drainage basins, a method to quantify connectivity based on graph theory was proposed. Traits of graph based stream networks, developed from the presence or absence of individual stream connections, were evaluated to investigate connectivity dynamics as well as the influence of connectivity on streamflow and runoff response in three disparate catchments. It was observed that daily average streamflow and runoff responses were greater with greater connectivity. However, the characteristics of the increases in streamflow and runoff ratio with increased connectivity varied by sub-basin and were strongly influenced by land cover heterogeneity. Differing landscape elements and arrangements affect streamflow and runoff response in different ways. In particular, basin scale connectivity dynamics were driven by gatekeeper elements which played a defining role in maintaining or disrupting the connectivity of elements lying upstream. The type and placement of gatekeeper elements controlled their storage state and heavily influenced connectivity at larger scales. Gatekeeper function controlled both the presence of and flow through connections throughout the stream network and thus connectivity and streamflow at the basin scale.

Connectivity was observed to be important to streamflow and runoff response. However, key land cover traits controlled how increased connectivity influenced streamflow and runoff response in each basin. The implications of these findings are that accurate prediction of streamflow and runoff response in a heterogeneous drainage basin with dynamic connectivity will require both an account of the presence or absence of connections but also a differentiation of connection type and an incorporation of aspects of local function that control the flow through connections themselves.

ACKNOWLEDGEMENTS

This study was part of the IP3-Improved Processes and Parameterisation for Prediction in Cold Regions—Network. Funding for this project was provided by the Canadian Foundation for Climate and Atmospheric Sciences, the Natural Sciences and Engineering Research Council of Canada, the Garfield Weston Foundation, Indian and Northern Affairs Canada, and Environment Canada. Special thanks go to Kirby Ebel, May Guan, Newell Hedstrom, Shawne Kokelj, and Mag McCluskie for their help conducting field work. May Guan also provided valuable advice and data. Bob Reid and Kirby Ebel are acknowledged for providing access to supplementary data.

REFERENCES

Ali G, Roy A. 2009. Revisiting hydrological sampling strategies for an accurate assessment of hydrologic connectivity in humid temperate systems. *Geography Compass* **3**: 350–374.

Allan CJ, Roulet NT. 1994. Runoff Generation in Zero-Order Precambrian Shield Catchments: The stormflow response of a heterogeneous landscape. *Hydrological Processes* **8**: 369–388.

Ambroise B. 2004. Variable 'active' versus 'contributing' areas or periods: a necessary distinction. *Hydrological Processes* **18**: 1149–1155.

Bracken L, Croke J. 2007. The concept of hydrological connectivity and its contribution to understanding runoff-dominated geomorphic systems. *Hydrological Processes* **21**: 1749–1763.

Black PE. 1997. Watershed functions. *Journal of the American Water Resources Association* **33**: 1–11.

Buttle JM. 2006. Mapping first order controls on streamflow from drainage basins: the T^3 template. *Hydrological Processes* **20**: 3415–3422.

Buttle JM, Dillon PJ, Eerkes GR. 2004. Hydrologic coupling of slopes, riparian zones and streams: an example from the Canadian Shield. *Journal of Hydrology* **287**: 161–177.

Chartrand G. 1977. *Introductory Graph Theory*. Dover: New York.

Congalton RJ. 1991. A review of assessing the accuracy of classifications of remotely sensed data. *Remote Sensing of the Environment* **37**: 34–46.

Detty JM, McGuire KJ. 2010. Topographic controls on shallow groundwater dynamics: implications of hydrologic connectivity between hillslopes and riparian zones in a till mantled catchment. *Hydrological Processes* **24**: 2222–2236.

Dingman SL. 1973. Effects of permafrost on stream characteristics in the discontinuous permafrost zone of Central Alaska. In *Permafrost: North American Contribution to the Second International Conference*. National Academy of Sciences: Washington, DC; pp. 447–453.

Domenico PA, Schwartz W. 1998. *Physical and Chemical Hydrogeology*. Wiley: Toronto.

Ecosystem Classification Group. 2008. *Ecological Regions of the Northwest Territories-Taiga Shield*. Department of Environment and Natural Resources, Government of the Northwest Territories: Yellowknife, NT, Canada.

Fang X, Pomeroy JW, Westbrook CJ, Guo X, AG Minke, Brown T. 2010. Prediction of snowmelt derived streamflow in a wetland dominated prairie basin. *Hydrology and Earth System Sciences* **14**: 991–1006.

Goodwin B. 2003. Is landscape connectivity a dependent or independent variable? *Landscape Ecology* **8**: 687–699.

Granger RJ, Hedstrom N. 2010. Controls on open water evaporation. *Hydrology and Earth Systems Sciences Discussions* **7**: 2709–2726.

Gross JS, Yellen J. 2006. *Graph Theory and Its Applications*. Chapman and Hall/CRC: New York.

Guan XJ, Spence C, Westbrook CJ. 2010. "Shallow soil moisture—ground thaw interactions and controls: 2. Influences of water and energy fluxes", *Hydrology and Earth System Sciences* **14**: 1387–1400.

Heron R, Woo MK. 1978. Snowmelt computation for a High Arctic site. Proceedings 35th Eastern Snow Conference, Hanover, New Hampshire, pp. 162–172.

Horst TW. 1997. A simple formula for attenuation of eddy fluxes measured with first order response scalar sensors. *Boundary Layer Meteorology* **94**: 517–520.

James A, Roulet N. 2007. Investigating hydrological connectivity and its association with threshold change in runoff response in a temperate forested watershed. *Hydrological Processes* **21**: 3391–3408.

Jensco K, McGlynn B, Gooseff M, Wondzell S, Becala K, Marshall L. 2009. Hydrological connectivity between landscapes and streams: Transferring reach- and plot- scale understanding to the catchment scale. *Water Resources Research* **45**: 1–16.

Jencso KG, McGlynn BL, Gooseff MN, Bencala KE, Wondzell SM. 2010. Hillslope hydrologic connectivity controls riparian groundwater turnover: Implications of catchment structure for riparian buffering and stream water sources. *Water Resources Research* **46**: W10524 DOI:10510.11029/12009wr008818.

Kaimal JC, Finnigan JJ. 1994. *Atmospheric Boundary Layer Flows—Their Structure and Measurement*. Oxford University Press: New York.

Kerr DE, Wilson P. 2000. Preliminary surficial geology studies and mineral exploration consideration in the Yellowknife area, Northwest Territories. Geological Survey of Canada, Current Research 2000-C3, p. 8.

Kindlmann P, Burel F. 2008. Connectivity measures: a review. *Landscape Ecology* **23**: 879–890.

Lane SN, Reaney SM, Heathwaite AL. 2009. Representation of landscape hydrological connectivity using a topographically driven surface flow index. *Water Resources Research* **45**: W08423, DOI:08410·01029/02008Wwr007336.

Lehmann P, Hinz C, McGrath G, Tromp-van Meerveld HJ, McDonnell JJ. 2007. Rainfall threshold for hillslope outflow: an emergent property of flow pathway connectivity. *Hydrology and Earth System Sciences* **11**: 1047–1063.

Massman WJ. 2000. A simple method for estimating frequency response corrections for eddy covariance systems. *Agricultural and Forest Meteorology* **104**: 185–198.

McFeeters SK. 1996. The use of normalized difference water index (NDWI) in the delineation of open water features. *International Journal of Remote Sensing* **7**: 1425–1432.

McGuire KJ, McDonnell JJ. 2010. Hydrological connectivity of hillslopes and streams: characteristic time scales and nonlinearities. *Water Resources Research* **46**: W10543, DOI:10510·11029/12010wr009341.

McNamara JP, Kane DL, Hinzman LD. 1998. An analysis of stream flow hydrology in the Kuparuk river basin, Arctic Alaska: a nested watershed approach. *Journal of Hydrology* **206**: 39–57.

Mielko C, Woo MK. 2006. Snowmelt runoff processes in a headwater lake and its catchment, subarctic Canadian Shield. *Hydrological Processes* **20**: 987–1000.

Pomeroy JW, Gray DM, Brown T, Hedstrom NR, Quinton WL, Granger RJ, Carey SK. 2007. The cold regions hydrological model: a platform for basing process representation and model structure on physical evidence. *Hydrological Processes* **21**: 2650–2667.

Pomeroy JW, Toth B, Granger RJ, Hedstrom NR, Essery RLH. 2003. Variation in surface energetics during snowmelt in complex terrain. *Journal of Hydrometeorology* **4**: 702–716.

Quinton W, Carey S. 2008. Towards an energy-based runoff generation theory for tundra landscapes. *Hydrological Processes* **22**: 4649–4653.

Quinton W, Hayashi M, Pietroniro A. 2003. Connectivity and storage functions of channel fens and flat bogs in northern basins. *Hydrological Processes* **17**: 3665–3684.

Reaney S, Bracken L, Kirkby M. 2006. Use of the connectivity of runoff model (CRUM) to investigate the influence of storm characteristics on runoff generation and connectivity in semi-arid areas. *Hydrological Processes* **7**: 894–906.

Sahimi M. 1984. *Applications of Percolation Theory*. Taylor and Francis: London.

Schröder B. 2006. Pattern, process, and function in landscape ecology and catchment hydrology—how can quantitative landscape ecology support predictions in ungauged basins? *Hydrological Earth Systems Sciences* **10**: 967–979.

Spence C. 2006. Hydrological processes and stream flow in a lake dominated watercourse. *Hydrological Processes* **20**: 3665–3681.

Spence C. 2007. On the relation between dynamic storage and runoff: A discussion on thresholds, efficiency, and function. *Water Resources Research* **43**: 1–11.

Spence C. 2010. A paradigm shift in hydrology: Storage thresholds across scales influence catchment runoff generation. *Geography Compass* **4**: 819–833.

Spence C, Guan XJ, Phillips R, Hedstrom N, Granger R, Reid B. 2010. Storage dynamics and streamflow in a catchment with a variable contributing area. *Hydrological Processes* **24**: 2209–2221.

Spence C, Woo MK. 2006. Hydrology of subarctic Canadian Shield: Heterogeneous headwater basins. *Journal of Hydrology* **317**: 138–154.

Stauffer D, Ahorony A. 1994. *Introduction to Percolation Theory*. Taylor and Francis: London.

Tromp van-Meerveld HJ, McDonnell JJ. 2006. Threshold relations in subsurface stormflow: 2. the fill and spill hypothesis. *Water Resources Research* **42**: 1–11.

Urban D, Keitt T. 2001. Landscape connectivity: a graph-theoretical perspective. *Ecology* **82**: 1205–1218.

Webb EK, Pearman GI, Leuning R. 1980. Correction of flux measurements for density effects due to heat and water vapour transfer. *Quaterly Journal of the Royal Meteorological Society* **106**: 85–100.

Western A, Blöschl G, Grayson R. 2001. Toward capturing hydrologically significant connectivity in spatial patterns. *Water Resources Research* **37**: 83–97.

Wolfe SA. 1998. Living with Frozen Ground: A Field Guide to Permafrost in Yellowknife Northwest Territories. Geological Survey of Canada Miscellaneous Report 64. p. 71.

Woo MK, Mielko C. 2007. An integrated framework of lake-stream connectivity for a semi-arid, subarctic environment. *Hydrological Processes* **21**: 2668–2674.

Xu H. 2006. Modification of normalized difference water index to enhance open water features in remotely sensed imagery. *International Journal of Remote Sensing* **14**: 3025–3033.

